






Quantitative study of the popliteal fossa in the human foetus

Mateusz Badura¹, Maria Dąbrowska¹, Anna Badura², Monika Paruszevska-Achtel¹, Magdalena Grzonkowska¹, Mariusz Baumgart¹, Michał Szpinda^{1, 3}

¹Department of Normal Anatomy, Collegium Medicum in Bydgoszcz, Nicolaus Copernicus University in Toruń, Bydgoszcz, Poland

²Department of Biopharmacy, Ludwik Rydygier Collegium Medicum in Bydgoszcz, Nicolaus Copernicus University in Toruń, Bydgoszcz, Poland

³Medical Faculty, Academy of Applied Medical and Social Sciences, Elbląg, Poland

[Received: 16 November 2023; Accepted: 28 December 2023; Early publication date: 22 January 2024]

The popliteal fossa presents an extensive diamond-shaped topographical element on the posterior aspect of the knee. With the use of classical anatomical dissection, digital image analysis of NIS Elements AR 3.0, and statistics, we morphometrically analysed the size of the popliteal fossa in human fetuses aged 17–29 weeks of gestation. Morphometric parameters of the popliteal fossa increased logarithmically with foetal age: $y = -44.421 + 24.301 \times \ln(\text{age})$ for length of superomedial boundary, $y = -41.379 + 22.777 \times \ln(\text{age})$ for length of superolateral boundary, $y = -39.019 + 20.981 \times \ln(\text{age})$ for inferomedial boundary, $y = -37.547 + 20.319 \times \ln(\text{age})$, for length of inferolateral boundary, $y = -28.915 + 15.822 \times \ln(\text{age})$ for transverse diameter, $y = -69.790 + 38.73 \times \ln(\text{age})$ for vertical diameter and $y = -485.631 + 240.844 \times \ln(\text{age})$ for projection surface area. Out of the 4 angles of the popliteal fossa the medial one was greatest, the inferior one the smallest, while the lateral one was somewhat smaller than the medial one and approximately 3 times greater than the superior one, with no difference with foetal age. In terms of morphometric parameters, the popliteal fossa in the human foetus displays neither male-female nor right-left differences. In the popliteal fossa, growth patterns of its 4 boundaries, vertical and transverse diameters, and projection surface area all follow natural logarithmic functions. All the morphometric data are considered age-specific reference intervals, which may be conducive in the diagnostics of congenital abnormalities in the human foetus. (Folia Morphol 2024; 83, 4: 845–857)

Keywords: popliteal fossa, gastrocnemius muscle, semitendinosus muscle, semimembranosus muscle, plantaris muscle, biceps femoris muscle, human foetus

INTRODUCTION

The popliteal fossa presents an extensive topographical element on the posterior aspect of the knee, included between flexor muscles of the thigh

and flexor muscles of the leg. The external contour of the popliteal fossa is diamond-shaped and covered with the popliteal fascia, which constitutes the roof of the popliteal fossa [1, 27]. The popliteal fossa

Address for correspondence: Mateusz Badura, Department of Normal Anatomy, Collegium Medicum in Bydgoszcz, Nicolaus Copernicus University in Toruń, ul. Łukasiewicza 1, 85–821 Bydgoszcz, Poland; e-mail: m.badura@cm.umk.pl

This article is available in open access under Creative Commons Attribution-Non-Commercial-No Derivatives 4.0 International (CC BY-NC-ND 4.0) license, allowing to download articles and share them with others as long as they credit the authors and the publisher, but without permission to change them in any way or use them commercially.

is bounded superomedially by the semitendinosus and semimembranosus muscles, superolaterally — by the biceps femoris muscle, inferomedially — by the medial head of the gastrocnemius muscle, and inferolaterally — by the lateral head of gastrocnemius muscle and plantaris muscle [10, 25, 27, 30]. All the aforementioned muscles flex and stabilise the knee joint [18, 25]. Apart from this, the semitendinosus muscle, semimembranosus muscle, and lateral head of the gastrocnemius muscle all medially rotate the leg (endorotation), while the biceps femoris muscle and medial head of the gastrocnemius are responsible for its lateral rotation (exorotation) [25, 27].

It should be emphasised that the floor of popliteal fossa is considerably greater than its roof. This is because the floor of the popliteal fossa extends as high as the adductor hiatus and as low as the tendinous arch of the soleus muscle [25, 27]. The floor of the popliteal fossa is composed of the popliteal surface of the femur, the articular capsule of the knee joint with its oblique popliteal ligament, and the popliteus muscle. According to Benniger and Delamarter [4], the oblique popliteal ligament is the very first constituent of the trifurcation of the semimembranosus tendon, and so it should be renamed the oblique popliteal tendon or expansion. The second expansion of this trifurcation ends on the anteroinferior aspect of the medial condyle of the tibia, the medial meniscus, and the medial collateral ligament of the knee, while the third one inserts onto the posteroinferior aspect of the medial condyle of the tibia and provides fibres to the individual fascia of the popliteus muscle.

The popliteal fossa communicates anteriorly through the adductor hiatus with the adductor canal. Superiorly, the popliteal fossa is freely continuous with the flexor compartment of the thigh. Of note, the soleus muscle resembles a kind of diaphragm by separating the popliteal fossa from the deep part of flexor compartment of the leg. Distally, the popliteal fossa communicates anteriorly with the extensor compartment of the leg due to the opening above the interosseous membrane of the leg that transmits the anterior tibial artery and veins. Deep to the tendinous arch of soleus muscle, both the tibial nerve and posterior tibial vessels leave the popliteal fossa and enter the deep part of the flexor compartment of the leg [4, 25, 27]. The posterolateral corner of the knee is largely stabilised by the biceps femoris muscle, the head of the fibula, the tendon of the popliteus muscle, and the popliteofibular ligament [9, 27]. Of note, there

is also the plantaris muscle, which is a small vestigial muscle with an incidence of 80–93% [17, 21, 24].

The popliteal fossa is traversed vertically by the popliteal artery and vein, both encompassed by the popliteal sheath. At the superior angle of popliteal fossa, the sciatic nerve externally divides into the tibial and common fibular nerves. Not being included in the popliteal sheath, the tibial nerve freely winds from lateral to medial on the posterior aspect of the popliteal vessels. The common fibular nerve traverses from the superior to the lateral angle of the popliteal fossa, and after leaving the popliteal fossa at the level of the neck of the fibula it divides into the superficial and deep fibular nerves [8, 27]. The popliteal fossa accommodates the popliteal lymph nodes, of which the middle popliteal lymph nodes clothe the popliteal vessels, the articular popliteal lymph node is between the oblique popliteal ligament and the popliteal artery, while the saphenous popliteal lymph node adheres to the junction of the small saphenous vein with the popliteal vein [17, 24, 25, 27].

The muscles limiting the popliteal fossa may indicate relevant variations, characterised by anomalous muscle slips that cross neurovascular structures and cause entrapment syndromes. The third head of gastrocnemius joining its medial head is most frequently quoted as producing such clinical problems [1, 10]. On the other hand, Liu et al. [18] presented the coexistence of bilateral absence of both the semimembranosus and quadratus femoris muscles.

After reviewing the professional literature, we failed to find any morphometrical data concerning the popliteal fossa in the human foetus. Thus, we decided to morphometrically analyse the size of the popliteal fossa in human foetuses aged 17 to 29 weeks of gestation with the use of objective methods: digital image analysis and statistics. The present study provides new detailed numerical data of the popliteal fossa, to thoroughly understand its growth dynamics.

With relation to the popliteal fossa, we aimed to examine the following:

- the possible variability of the muscles limiting the popliteal fossa that may considerably influence its morphometrical parameters;
- its size by performing its linear and planar measurements in order to achieve age-specific reference intervals of examined parameters;
- the possible right-left and male-female differences in all examined parameters; and
- growth patterns for all examined parameters.

Table 1. Characteristics of the examined foetal sample with its distribution regarding age, number, and sex.

Gestational age	Crown-rump length [mm]		Number of fetuses	Sex	
	Weeks	Mean		SD	♂
17	117.5	0.707	2	2	
18	136.5	7.778	2	1	1
19	151	2.517	3	2	1
20	167	1.414	2	1	1
21	176	3.512	3	2	1
22	182.5	0.707	2		2
23	195	4.243	2		2
24	211.5	0.707	2	1	1
25	216.5	2.121	2	1	1
26	231	2.828	2	1	1
27	241.4	2.121	2	1	1
28	247.5	1.708	4	1	3
29	260.5	0.707	3	1	2
Total			31	14	17

SD — standard deviation.

MATERIALS AND METHODS

The examined material comprised 31 fetuses of both sexes, 17 males and 14 females, at the age of 17 to 29 weeks of gestation, derived from spontaneous miscarriages and preterm deliveries. The foetal collection was from our Department of Normal Anatomy. The present examinations were approved by the Bioethics Committee of the Ludwik Rydygier Collegium Medicum in Bydgoszcz, and the Nicolaus Copernicus University in Bydgoszcz. The foetal ages were determined on the basis of the crown-rump length. Table 1 presents the characteristics of the examined foetal samples with their distribution regarding age, number, and sex.

With the use of classical anatomical dissection on the posterior aspect of the lower limb, the popliteal fossa was bilaterally exposed. The photographic documentation of the popliteal fossae was prepared using a Canon EOS 70D(W), while for the morphometric analysis the NIS Elements AR 3.0 system was used. For each popliteal fossa, the following 11 parameters were defined and measured (Fig. 1A–C):

- length of superomedial boundary (mm), extending between the superior and medial angles of the popliteal fossa along the semitendinosus muscle;
- length of superolateral boundary (mm), extending between the superior and lateral angles of the popliteal fossa along the biceps femoris muscle;

- length of inferomedial boundary (mm), extending between the inferior and medial angles of the popliteal fossa along the medial head of gastrocnemius muscle;
- length of the inferolateral boundary (mm), extending between the inferior and lateral angles of the popliteal fossa along the lateral head of the gastrocnemius muscle;
- transverse diameter (mm), extending between the medial and lateral angles of the popliteal fossa;
- vertical diameter (mm), extending between the superior and inferior angles of the popliteal fossa;
- projection surface area (mm²), calculated semiautomatically after the popliteal fossa was outlined;
- superior angle (α) of popliteal fossa, between the semitendinosus and biceps femoris muscles;
- medial angle (β) of popliteal fossa, between the semitendinosus muscle and medial head of gastrocnemius muscle;
- inferior angle (γ) of popliteal fossa, between the medial and lateral heads of gastrocnemius muscle; and
- lateral angle (δ) of popliteal fossa, between the lateral head of the gastrocnemius muscle and the biceps femoris muscle.

All numerical data were subject to statistical analysis with the use of STATISTICA 13.0. Because of the normal distribution of numerical data, our results have been presented as means and standard deviations (SD). To compare right-left means and male-female means, Student's t-test for dependent variables and Student t-test for independent variables were respectively used with one-way analysis of variance. The growth patterns of particular morphometrical parameters were examined using linear and nonlinear regression analyses. The growth dynamics of best fit was unequivocally characterised and selected by the greatest value of its coefficient of determination (R^2). Statistically significant differences were considered at $p < 0.05$.

RESULTS

In the study material we found no variability concerning the skeletal muscles limiting the popliteal fossa, namely the semitendinosus, semimembranosus, biceps femoris, plantaris, and gastrocnemius muscles that all follow typically without extra muscle slips. As a result, the shape of each popliteal fossa was regular and diamond shaped.

The statistical analysis did not show any statistically significant male-female differences for all the

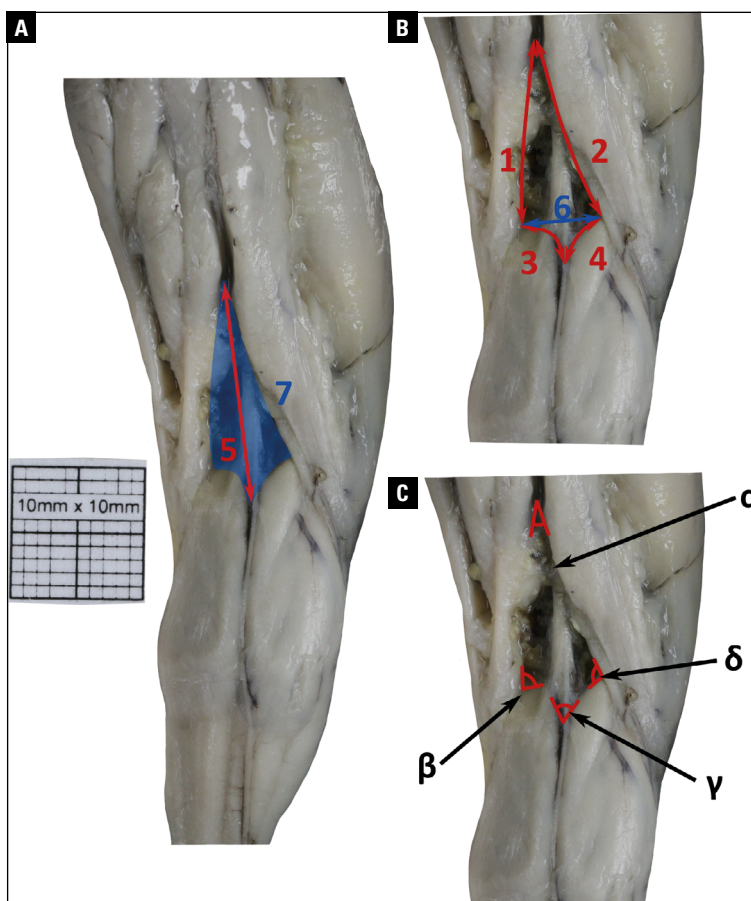


Figure 1. The popliteal fossa in a female foetus at 22 weeks showing the measured parameters (A–C); 1 — length of superomedial boundary; 2 — length of superolateral boundary; 3 — length of inferomedial boundary; 4 — length of inferolateral boundary; 5 — vertical diameter; 6 — transverse diameter; 7 — projection surface area; superior (α) angle, medial (β) angle, inferior (γ) angle, and lateral (δ) angle of popliteal fossa.

Table 2. Regression analysis for examined parameters of the popliteal fossa with age.

Parameter	Regression formulae related to age	R ²	F	P
Superomedial border [mm]	$y = -44.421 + 24.301 \times \ln(\text{age})$	0.897	535.1	= 0.00
Superolateral border [mm]	$y = -41.379 + 22.777 \times \ln(\text{age})$	0.862	377.2	= 0.00
Inferomedial border [mm]	$y = -39.019 + 20.981 \times \ln(\text{age})$	0.911	614.5	= 0.00
Inferolateral border [mm]	$y = -37.547 + 20.319 \times \ln(\text{age})$	0.860	369.6	= 0.00
Length [mm]	$y = -69.790 + 38.730 \times \ln(\text{age})$	0.901	548.7	= 0.00
Width [mm]	$y = -28.915 + 15.822 \times \ln(\text{age})$	0.780	213.3	= 0.00
Surface area [mm ²]	$y = -485.631 + 240.844 \times \ln(\text{age})$	0.936	879.0	= 0.00

parameters studied ($p > 0.05$), thus allowing us to aggregate them, without regard to sex (Tab. 2–6).

Length values of the 4 boundaries of the popliteal fossa presented the following decreasing sequence: the superomedial, superolateral, inferolateral, and inferomedial ones.

The mean length of the superomedial boundary of the popliteal fossa (Tab. 3A) increased from 6.205 ± 0.219 mm at week 17 to 15.221 ± 0.382 mm at week 29 of gestation on the right, and from 6.321 ± 0.099 to 14.935 ± 0.106 mm, respectively, without right-left differences ($p > 0.05$). In the analysed period the mean length of the superomedial boundary of the popliteal fossa followed the natural logarithmic function $y = -44.421 + 24.301 \times \ln(\text{age})$ with $R^2 = 0.897$ (Fig. 2A).

At the ages of 17–29 weeks of gestation, the mean length of the superolateral boundary of the popliteal fossa (Tab. 3A) increased its value from 5.395 ± 0.064 to 13.145 ± 0.106 mm on the right and from 5.54 ± 0.028 to 13.225 ± 0.219 mm on the left, without right-left differences ($p > 0.05$). The mean length

Table 3A. Statistical analysis of numerical data of the length of superomedial and superolateral boundary (mean \pm SD) of the popliteal fossa.

Gestational age [weeks]	Number of fetuses	Length of superomedial boundary				Length of superolateral boundary			
		Right		Left		Right		Left	
		Mean	SD	Mean	SD	Mean	SD	Mean	SD
17	2	6.205	0.219	6.320	0.099	5.395	0.064	5.540	0.028
18	2	6.875	0.191	6.945	0.021	6.040	1.457	6.045	1.407
19	3	9.230	1.127	9.550	1.190	8.820	1.134	9.110	1.169
20	2	9.745	0.926	9.765	0.841	10.495	0.530	9.995	0.078
21	3	10.270	0.242	10.980	0.554	10.27	0.806	10.650	0.860
		(p < 0.01)				(p < 0.01)			
22	2	10.115	0.106	10.540	0.099	10.575	0.488	10.175	0.219
23	2	11.525	0.658	12.000	0.226	10.350	0.523	10.925	0.954
24	2	11.410	0.778	10.680	0.481	10.445	0.290	10.885	0.035
25	2	10.635	0.573	10.945	0.672	10.715	0.530	10.175	0.205
26	2	11.870	0.014	11.500	0.608	12.785	0.346	12.290	0.438
		(p < 0.01)				(p < 0.01)			
27	2	13.035	0.643	13.380	0.848	12.845	0.346	13.085	0.021
28	4	14.570	0.360	14.715	0.184	13.765	0.396	13.320	0.454
29	3	15.220	0.382	14.935	0.106	13.145	0.106	13.225	0.219
		(p < 0.01)				(p < 0.01)			

Table 3B. Statistical analysis of numerical data of the length of inferomedial and inferolateral boundary (mean \pm SD) of the popliteal fossa.

Gestational age [weeks]	Number of fetuses	Length of inferomedial boundary				Length of inferolateral boundary			
		Right		Left		Right		Left	
		Mean	SD	Mean	SD	Mean	SD	Mean	SD
17	2	4.720	0.212	4.755	0.007	5.340	0.028	5.765	0.262
18	2	5.940	0.127	5.900	0.042	6.340	1.061	5.955	0.559
19	3	6.910	0.590	6.450	0.757	6.070	0.569	6.470	0.974
20	2	7.410	0.976	7.320	1.541	7.720	1.626	7.365	2.213
21	3	8.810	0.378	8.790	0.796	8.180	0.700	9.020	0.523
		(p < 0.01)				(p < 0.01)			
22	2	7.845	0.247	7.995	0.785	7.125	0.559	7.060	0.325
23	2	8.740	0.580	9.030	0.424	8.655	0.672	9.185	0.855
24	2	8.800	1.131	8.880	1.188	8.220	0.594	8.465	0.728
25	2	9.545	0.516	9.575	0.318	9.630	0.283	9.860	0.184
26	2	10.215	0.389	10.155	0.530	10.035	0.629	10.110	0.877
		(p < 0.01)				(p < 0.01)			
27	2	10.735	0.290	10.685	0.474	11.695	0.049	11.305	0.389
28	4	11.245	0.258	11.390	0.352	11.365	1.306	11.470	0.906
29	3	13.195	0.361	13.320	0.424	11.530	0.184	11.640	0.085
		(p < 0.01)				(p < 0.01)			

SD — standard deviation.

of the superolateral boundary of the popliteal fossa modelled the natural logarithmic function $y = -41.379 + 22.777 \times \ln(\text{age})$ with $R^2 = 0.862$ (Fig. 2B).

Between weeks 17 and 29, the mean length of the inferomedial boundary of the popliteal fossa (Tab. 3B) grew from 4.723 ± 0.212 to 13.195 ± 0.360 mm on

Table 4. Statistical analysis of numerical data of the vertical and transverse diameters (mean ± SD) of the popliteal fossa.

Gestational age [weeks]	Number of fetuses	Vertical diameter [mm]				Transverse diameter [mm]			
		Right		Left		Right		Left	
		Mean	SD	Mean	SD	Mean	SD	Mean	SD
17	2	10.665	0.488	10.765	0.021	4.530	0.071	4.695	0.035
18	2	11.745	0.389	11.605	0.304	5.155	0.205	5.190	0.297
19	3	14.420	0.734	14.130	0.784	5.030	0.358	5.060	0.325
20	2	17.245	1.492	16.455	1.195	5.020	0.679	4.835	0.318
21	3	17.290	1.124	18.160	1.200	7.050	1.603	6.810	0.111
		(p < 0.01)				(p < 0.01)			
22	2	17.350	0.891	17.140	0.749	6.260	0.509	6.130	0.551
23	2	19.600	0.085	20.130	0.523	6.790	0.042	6.600	0.382
24	2	19.015	0.276	18.680	0.594	7.635	1.534	7.560	2.164
25	2	21.495	1.421	20.845	0.671	8.510	0.099	8.865	0.035
26	2	22.515	3.472	22.050	1.457	8.460	0.198	8.475	0.403
		(p < 0.01)				(p < 0.01)			
27	2	21.335	1.860	20.975	1.619	9.680	0.113	9.460	0.622
28	4	24.055	0.044	24.075	0.561	8.400	0.290	8.235	0.191
29	3	23.035	0.544	22.695	0.502	10.735	0.191	10.890	0.184
		(p < 0.01)				(p < 0.01)			

SD — standard deviation.

Table 5. Statistical analysis of numerical data of the projection surface area (mean ± SD) of the popliteal fossa.

Gestational age (weeks)	Number of fetuses	Projection surface area [mm ²]			
		Right		Left	
		Mean	SD	Mean	SD
17	2	28.380	0.707	29.485	0.898
18	2	34.620	1.669	34.485	1.761
19	3	38.550	0.959	38.030	0.836
20	2	38.760	0.382	38.185	0.092
21	3	45.720	0.692	44.160	1.317
		(p < 0.01)			
22	2	49.225	0.785	48.380	0.848
23	2	63.535	5.537	62.370	5.614
24	2	73.110	6.307	70.055	2.779
25	2	70.855	0.969	72.290	2.744
26	2	78.910	0.042	80.065	2.595
		(p < 0.01)			
27	2	92.895	16.440	91.605	13.781
28	4	101.055	3.107	99.720	3.661
29	3	101.600	1.527	101.195	0.219
		(p < 0.01)			

SD — standard deviation

the right and from 4.755 ± 0.007 to 13.320 ± 0.424 mm on the left, without right-left differences (p > 0.05). The mean length of inferomedial boundary

of popliteal fossa computed the natural logarithmic function $y = -39.019 + 20.981 \times \ln(\text{age})$ with $R^2 = 0.911$ (Fig. 2C).

The mean length of the inferolateral boundary of the popliteal fossa (Tab. 3B) revealed an increase in values from 5.34 ± 0.028 mm at week 17 to 11.53 ± 0.184 mm at week 29 on the right, and correspondingly from 5.765 ± 0.262 to 11.64 ± 0.849 mm on the left, without right-left differences (p > 0.05). The mean length of inferolateral boundary of popliteal fossa generated the natural logarithmic function $y = -37.547 + 20.319 \times \ln(\text{age})$ with $R^2 = 0.860$ (Fig. 2D).

The vertical diameter of the popliteal fossa was approximately twice its transverse diameter. Between weeks 17 and 29 of gestation the mean transverse diameter of the popliteal fossa (Tab. 4) grew from 4.532 ± 0.070 to 10.735 ± 0.190 mm on the right and from 4.695 ± 0.035 to 10.891 ± 0.184 mm on the left, without right-left differences (p > 0.05). The mean transverse diameter of popliteal fossa followed the natural logarithmic function $y = -28.915 + 15.822 \times \ln(\text{age})$, with $R^2 = 0.780$ (Fig. 2F).

The mean vertical diameter of popliteal fossa (Tab. 4) increased from 10.665 ± 0.488 mm at week 17 to 23.035 ± 0.544 mm at week 29 on the right, and correspondingly from 10.765 ± 0.021 to 22.695 ±

Table 6. Statistical analysis of numerical data of the 4 angles (mean \pm SD) of the popliteal fossa.

Gestational age [weeks]	Number of foetuses	Superior (α) angle				Medial (β) angle				Inferior (γ) angle				Lateral (δ) angle			
		Right		Left		Right		Left		Right		Left		Right		Left	
		Mean	SD	Mean	SD	Mean	SD	Mean	SD	Mean	SD	Mean	SD	Mean	SD	Mean	SD
17	2	38.17	0.707	42.075	6.230	134.66	5.508	141.08	12.098	34.85	10.797	22.60	2.446	133.89	8.534	136.4	2.659
18	2	36.53	7.001	36.655	7.163	134.30	7.530	130.33	6.484	34.08	10.472	44.77	1.704	126.28	3.649	133.72	0.035
19	3	39.65	4.643	39.65	5.282	129.04	1.0515	129.66	0.647	44.72	5.284	45.98	0.911	136.57	2.232	136.48	2.391
20	2	35.19	4.101	36.045	1.167	141.96	2.121	137.90	3.443	40.18	1.485	39.30	0.735	137.74	6.117	138.31	8.429
21	3	37.99	2.598	36.22	2.782	139.35	6.736	138.44	9.031	39.82	3.165	39.74	3.621	141.76	5.488	141.88	4.631
				($p < 0.01$)			($p < 0.01$)				($p < 0.01$)					($p < 0.01$)	
22	2	35.25	5.565	36.30	3.989	142.53	3.811	141.93	3.234	45.67	2.170	47.28	5.374	132.64	4.264	135.98	0.480
23	2	37.29	5.728	40.535	2.552	141.85	7.170	140.71	8.019	40.23	2.984	40.45	1.414	146.55	4.229	138.54	4.080
24	2	37.06	6.993	35.20	5.756	134.47	9.291	135.43	9.376	43.28	3.854	43.81	1.627	133.96	8.026	134.75	7.658
25	2	32.95	2.270	31.665	1.902	144.17	2.340	145.85	0.035	38.30	0.460	38.80	1.167	141.77	5.105	141.98	4.808
				($p < 0.01$)			($p < 0.01$)				($p < 0.01$)					($p < 0.01$)	
26	2	37.11	2.998	39.13	7.085	144.36	0.990	144.81	2.107	33.11	8.959	31.86	10.628	136.52	10.394	132.39	1.407
27	2	40.46	1.506	39.22	0.297	144.14	5.883	144.09	6.123	39.08	0.424	38.80	0.841	132.82	2.008	134.02	1.725
28	4	36.06	3.573	37.96	3.474	137.91	4.658	141.91	1.719	38.84	3.462	37.29	4.768	145.30	4.305	141.15	2.886
29	3	39.40	0.007	40.50	0.693	137.83	3.019	137.66	1.846	40.43	0.4957	40.47	0.778	135.58	1.895	136.32	1.527
				($p < 0.01$)			($p < 0.01$)				($p < 0.01$)					($p < 0.01$)	

SD — standard deviation.

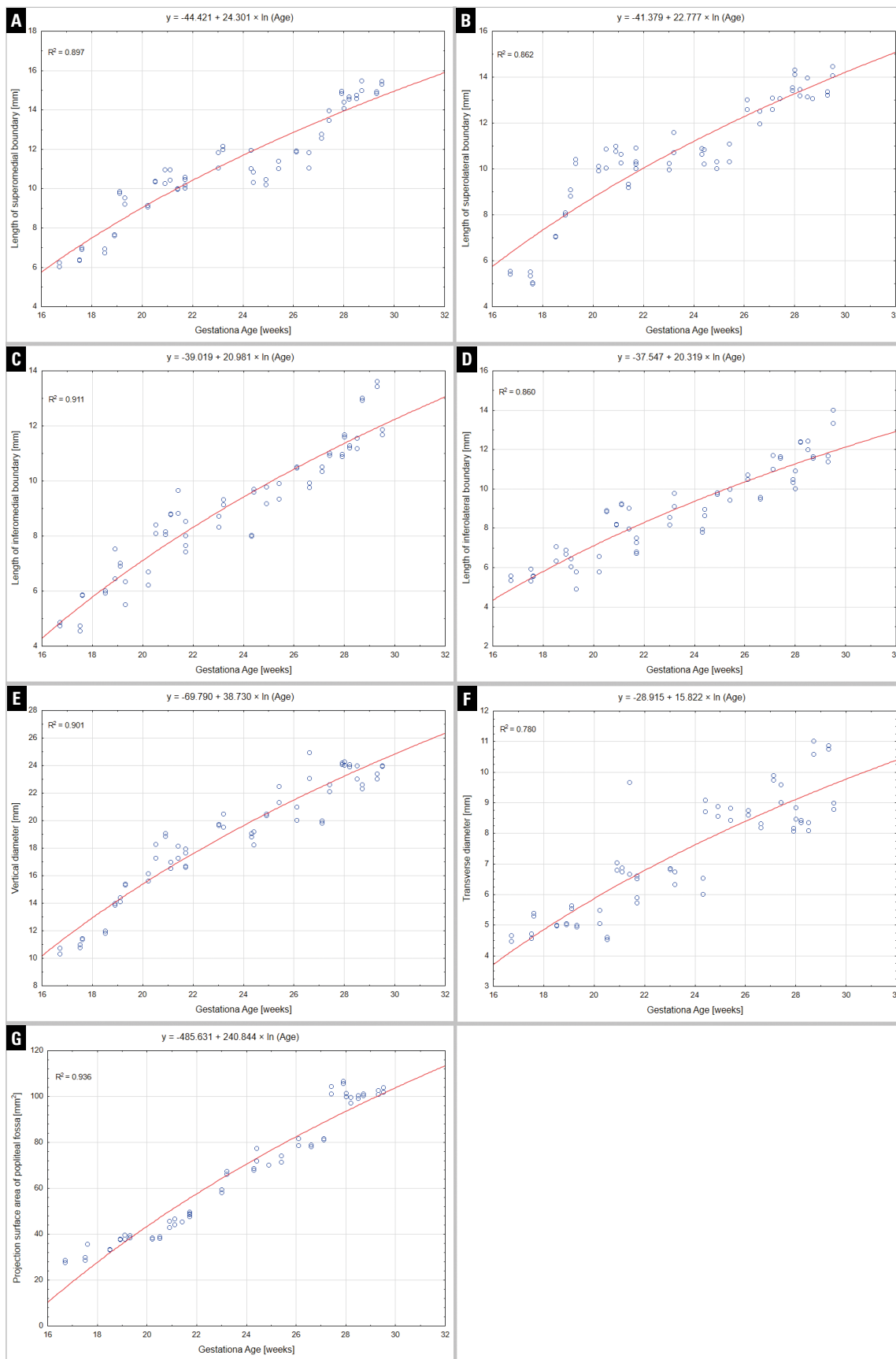


Figure 2. Regression lines for the length of superomedial boundary (A), superolateral boundary (B), inferomedial boundary (C), inferolateral boundary (D), vertical diameter (E), transverse diameter (F), and projection surface area (G) of the popliteal fossa.

± 0.502 mm on the left. In the analysed period the mean vertical diameter of popliteal fossa displayed the natural logarithmic function $y = -69.790 + 38.73 \times \ln(\text{age})$, with $R^2 = 0.901$ (Fig. 2E).

At the age range of 17–29 weeks, the mean projection surface area of the popliteal fossa (Tab. 5) grew from 28.381 ± 0.707 to 101.195 ± 0.220 mm² on the right, and from 29.485 ± 0.898 to 101.195 ± 0.220 mm² on the left. The mean projection surface area of popliteal fossa modelled the natural logarithmic function $y = -485.631 + 240.844 \times \ln(\text{age})$, with $R^2 = 0.936$ (Fig. 2G).

The 4 angles of the popliteal fossa presented the following decreasing sequence: medial, lateral, superior, and inferior. Their values did not significantly change with foetal age ($p > 0.05$).

The mean superior (α) angle of the popliteal fossa (Tab. 6) between weeks 17 and 29 ranged from $38.172 \pm 0.707^\circ$ to $39.405 \pm 0.007^\circ$ on the right, and from $42.075 \pm 6.230^\circ$ to $40.500 \pm 0.692^\circ$ on the left, without statistically significant differences on either side or between the left and right sides. At the same time, the mean medial (β) angle of popliteal fossa (Tab. 6) ranged from $141.085 \pm 12.099^\circ$ to $137.665 \pm 1.846^\circ$ on the right, and from $134.665 \pm 5.509^\circ$ to $137.835 \pm 3.019^\circ$ on the left, without statistically significant differences on either side and between the left and right sides. The mean inferior (γ) angle of the popliteal fossa (Tab. 6) between weeks 17 and 29 changed from $24.855 \pm 10.798^\circ$ to $40.430 \pm 0.450^\circ$ on the right, and from $22.611 \pm 2.447^\circ$ to $40.470 \pm 2.447^\circ$ on the left, without statistically significant differences on either side and between left and right sides. The mean lateral (δ) angle of the popliteal fossa (Tab. 6) reached the values of $133.695 \pm 8.535^\circ$ at week 17 and $135.58 \pm 1.896^\circ$ at week 29 on the right, and, respectively, $136.412 \pm 2.659^\circ$ and $136.321 \pm 1.527^\circ$ on the left side, without statistically significant differences on either side or between left and right sides.

DISCUSSION

The present discussion was separated into the following 5 subdivisions: sex and laterality differences of the popliteal fossa and its limiting muscles; numerical data of the popliteal fossa in the growing human foetus; variability of the muscles limiting the popliteal fossa; morphometric studies of the muscles limiting the popliteal fossa in the human foetus; and clinical aspects of the popliteal fossa.

Sex and laterality differences of the popliteal fossa and its limiting muscles

In the material under examination, we found the size of the popliteal fossa to be independent of both the sex and laterality. Because we failed to find any morphometric study of the popliteal fossa in the professional literature, we could not develop a comprehensive discussion about the sex and laterality differences of the popliteal fossa. However, after reviewing the medical literature, we found the muscles limiting the popliteal fossa to be independent of sex and laterality. This referred to the plantaris muscle [24], the triceps surae muscle [15], the biceps femoris muscle [12], the semimembranosus muscle [2], and the semitendinosus muscle [3]. All the aforementioned muscles displayed a commensurate increase in length and width, expressed by linear growth patterns. Szpinda et al. [29] alone reported the only laterality differences with relation to the short head of the biceps femoris muscle. Neither sex nor laterality showed statistically significant differences in other skeletal muscles of the human foetus: the triceps brachii muscle [13], the biceps brachii muscle [28], and the rectus abdominis muscle [12] that extended typically from its origin to its insertion.

Numerical data of the popliteal fossa in the growing human foetus

Morphometric studies of the popliteal fossa may be helpful from both cognitive and clinical aspects. Dudek et al. [12] claimed that growing anatomical structures should be described accurately enough for clinical and prognostic purposes with segmental-linear models or one-function models. Furthermore, the degree of adjustment of model parameters and measurement results are strongly influenced by the function form, and especially by the size of anatomical structures. However, there are no reports in the professional literature to do with the size of the popliteal fossa in human foetuses. To the best of our knowledge, the present article is the first one to focus on the quantitative analysis on the popliteal fossa in the human foetus. Due to neither male-female nor right-left statistically significant differences ($p > 0.05$), we decided to aggregate numerical data concerning particular morphometric parameters and model only one growth pattern of statistical significance for each parameter. From a geometrical point of view, the diamond-shaped popliteal fossa presents a quadrangular with 4 sides and 2 diagonals. Having

compared lengths of 4 boundaries of the popliteal fossa, we found the superomedial one to be greatest, the inferomedial one to be smallest, and the superolateral one to be greater than the inferolateral one. In the material under examination, all these diameters elongate with foetal age in accordance with natural logarithmic functions. The lengths of the superomedial, inferomedial, superolateral, and inferolateral boundaries of the popliteal fossa modelled the following natural logarithmic functions: $y = -44.421 + 24.301 \times \ln(\text{age})$, $y = -39.019 + 20.981 \times \ln(\text{age})$, $y = -41.379 + 22.777 \times \ln(\text{age})$, and $y = -37.547 + 20.319 \times \ln(\text{age})$, respectively.

As it transpired, the vertical diameter of the popliteal fossa was roughly twice its transverse diameter. In the study period, both vertical and transverse diameters of the popliteal fossa displayed the natural logarithmic growths: $y = -69.790 + 38.73 \times \ln(\text{age})$ and $y = -28.915 + 15.822 \times \ln(\text{age})$, correspondingly. Furthermore, the projection surface area of popliteal fossa increased in accordance with the natural logarithmic function $y = -485.631 + 240.844 \times \ln(\text{age})$.

Out of the 4 angles of the popliteal fossa, the medial one was greatest, the inferior one the smallest, while the lateral one was somewhat smaller than the medial one and approximately 3 times greater than the superior one.

The mean superior (α) angle of the popliteal fossa (Tab. 6) between weeks 17 and 29 ranged from $38.172 \pm 0.707^\circ$ to $39.405 \pm 0.007^\circ$ on the right, and from $42.075 \pm 6.230^\circ$ to $40.500 \pm 0.692^\circ$ on the left, without statistically significant differences on either side or between left and right sides. Since the statistical analysis showed their values not to significantly change with foetal age ($p > 0.05$), we could not model their growth patterns.

Variability of the muscles limiting the popliteal fossa

In the material under examination, we did not find any variability of the skeletal muscles limiting the popliteal fossa: the semitendinosus, semimembranosus, biceps femoris, plantaris, and gastrocnemius muscles all extended in a typical fashion. Okamoto et al. [20] found an anomalous muscle originating from the medial head of gastrocnemius, passing transversely subjacent to the popliteal fascia, and crossing posteriorly to the neurovascular structures of the popliteal fossa to finally end on the biceps femoris tendon. Such an atypical muscle must have been derived from

the short head of the biceps femoris muscle because it was innervated by the common peroneal nerve. Kim et al. [16] presented a similar thin transverse muscle in the superficial region of the popliteal region that originated from the biceps femoris tendon and inserted onto the medial head of gastrocnemius muscle. It was innervated by a motor branch originating from the lateral sural cutaneous nerve and supplied by the sural artery.

The third head of the gastrocnemius muscle presents its most common variation [1, 5, 6, 10, 14], found in 1.7–5.5% of individuals [10]. The third head of the gastrocnemius muscle usually originates from the lateral epicondyle of femur, the lateral aspect of the popliteal surface of femur, and the articular capsule of the knee joint. It may sporadically originate from the long head of biceps femoris muscle, the lateral lip of linea aspera, the crural fascia, and even from the semitendinosus belly [5, 6, 10, 14]. The third head of the gastrocnemius muscle typically descends vertically subjacent to the popliteal fascia as the medial partner of the plantaris muscle, and it inserts onto the junction of the medial and lateral heads of the gastrocnemius muscle [10]. It may possess some separate origins and divide near its insertion to merge with the 2 heads of the gastrocnemius muscle. The biceps femoris muscle may either lack its short head or possess an extra head, originating from the ischial tuberosity, lateral lip of linea aspera, or the lateral epicondyle of femur. Sinav et al. [23] found atypical muscle slips that underlay the popliteal fascia and fascia lata, respectively. The first one arose from the inferior part of the long head of biceps femoris muscle and ended in the crural fascia, while the other started with the superior part of the long head of biceps femoris muscle and joined the semitendinosus muscle. Liu et al. [18] and Sussmann [26] reported the bilateral absence of the semimembranosus muscle. Chason et al. [7] observed the tensor fasciae suralis, the belly of which originated from the lateral aspect of the semitendinosus muscle and extended to the distal thigh. Its long tendon superficially crossed the superficial popliteal fossa, so as to merge with the most superficial part of the calcaneal tendon.

Morphometric studies of the muscles limiting the popliteal fossa in the human foetus

Dudek et al. [12] examined the growth dynamics of the biceps femoris muscle, which is the superolateral boundary of the popliteal fossa, in 67 human

foetuses of both sexes with a crown-rump length of 130–237 mm. Szpinda et al. [29] examined the biceps femoris muscle in 30 human foetuses aged 17–30 weeks of gestation. The growth of its long head followed commensurately in both length and width, and modelled linear functions: $y = -25.27 + 3.61 \times \text{age}$ ($R = 0.90$) and $y = -2.75 + 0.35 \times \text{age}$ ($R = 0.77$), respectively. Of note, the growth of the short head of the biceps femoris presented statistically significant right-left differences. Its length modelled the linear functions: $y = -10.09 + 1.86 \times \text{age}$ ($R = 0.79$) on the right and $y = -4.45 + 1.58 \times \text{age}$ ($R = 0.77$) on the left. Correspondingly, its width followed the linear functions: $y = -0.80 + 0.12 \times \text{age}$ ($R = 0.54$) on the right and $y = 0.73 + 0.04 \times \text{age}$ ($R = 0.25$) on the left. The length of tendon of biceps femoris muscle increase proportionately: $y = -9.85 + 1.41 \times \text{age}$ ($R = 0.90$). Kadir et al. [15] performed a morphometric study of the gastrocnemius muscle in terms of its length, width, and thickness in 51 human foetuses of both sexes aged 15–40 weeks of gestation. The medial head of gastrocnemius proved to be longer, wider, and thicker than the lateral one. During the study period the length of the medial and lateral heads of the gastrocnemius muscle increased from 28.01 to 80.89 mm and from 14.77 to 53.54 mm, respectively. Yildiz et al. [32] examined the length and width of the plantaris belly and tendon in 24 human foetuses aged 17–40 weeks of gestation. The plantaris muscle was absent unilaterally in one male foetus and bilaterally in one female foetus, while the remaining plantaris muscles were typically structured with a relatively short belly and long tendon. When comparing the plantaris belly in the second and third trimesters of gestation, its mean length increased from 7.48 to 17.58 mm, while its mean width increased from 2.96 to 5.82 mm. As far as the plantaris tendon is concerned in the second and third trimesters of gestation, its mean length increased from 36.30 to 65.39 mm, while its mean width increased from 0.43 to 0.95 mm.

Badura et al. [2] examined the growth dynamics of the semimembranosus muscle in the human foetus that presents the superomedial boundary of the popliteal fossa. Both the length and width of the semimembranosus tendon modelled linear functions: $y = 0.058 + 0.992 \times \text{age}$ ($R = 0.99$; $p < 0.05$) and $y = 0.068 + 0.940 \times \text{age}$ ($R = 0.98$; $p < 0.05$), respectively. Another study by Badura et al. [3] concentrated on the foetal growth of the semitendinosus muscle

that followed proportionately, as follows: $y = 9.8971 + 1.7803 \times \text{age}$ ($R = 0.9752$; $p < 0.05$) for length of the semitendinosus belly, $y = -0.5495 + 0.207 \times \text{age}$ ($R = 0.8729$; $p < 0.05$) for width of the semitendinosus belly, $y = -8.1735 + 1.4421 \times \text{age}$ ($R = 0.9401$; $p < 0.05$) for length of the semitendinosus tendon, and $y = 0.0097 + 0.0442 \times \text{age}$ ($R = 0.8833$; $p < 0.05$) for width of semitendinosus tendon.

Clinical aspects of the popliteal fossa

A thorough understanding of both the topography and contents of the popliteal fossa is critical in patients suffering from its injury and other pathologies [1]. Injuries of the popliteal fossa are sporadic, constitute only 2% of all surgical interventions around the knee, and mostly affect the plantaris muscle. Such a condition is clinically termed “tennis player’s leg” or “tennis leg” [21]. The injury of the plantaris muscle occurs most frequently while running or jumping and is caused by an eccentric load placed across the ankle with the extended knee [24]. Because of its long tendon and course with the calcaneal tendon, the plantaris muscle is commonly used for reconstruction of other tendons and ligaments, and it may contribute to Achilles tendinopathy [21]. Isolated or combined chronic injury of the posterolateral corner of popliteal fossa requires its reconstruction with reconstruction of any concomitant cruciate ligament injury [9]. Damage to the soleus muscle mostly results from running or springing and is characterised by a severe pain after breaks, including a night rest.

Supernumerary muscles positioned at the inferior part of the popliteal fossa constituted a much more frequent reason for entrapment of the popliteal vessels than those at the superior part of the popliteal fossa [6, 7, 14, 15, 19, 21]. The third head of the gastrocnemius muscle traverses the inferior part of the popliteal fossa and may exert a significant compressive effect on the adjacent neurovascular structures, usually resulting in popliteal vessel entrapment or compressive neuropathies, involving branches of the tibial and common fibular nerves [6, 10]. Partial resection of the third head of the gastrocnemius muscle is usually sufficient to relieve entrapped symptoms [14]. Kotian et al. [17] found a sporadic variation of the plantaris muscle to stem from a common origin with the further formation of 2 muscle bellies that crossed and entrapped the neurovascular bundle in the popliteal fossa. Olewnik et al. [21] presented an anomalous plantaris muscle that originated from

the knee joint capsule, crossed posterior to the tibial nerve and the popliteal vessels, and might potentially compress the tibial nerve. Entrapment syndromes are characterized by a leg pain, tenderness in the popliteal fossa and decreased pulsations of the posterior tibial and dorsalis pedis arteries.

Chason et al. [7] and Montet et al. [19] emphasised that the tensor fasciae suralis muscle presents a sporadic cause of a popliteal mass, which must be differentiated from other pathological masses. Anatomical variations of the muscles limiting the popliteal fossa may be valuable for the surgical approaches in popliteal vessel syndromes [1]. Monotonous micro-trauma of the pes anserinus, comprising tendons of the semitendinosus, gracilis, and sartorius muscles, may lead to chronic inflammation and later result in the development of degenerative changes in this region [22].

Neoplastic changes may be localised in the popliteal region. Weschenfelder et al. [31] presented a desmoid tumour at the right popliteal fossa of a 34-year-old woman. This tumour surrounded the lateral head of the gastrocnemius muscle, involved the common fibular nerve, and infiltrated the head of fibula as far as the posterolateral aspect of the articular capsule of knee joint. Derzsi et al. [11] described a haemangioma of the left popliteal fossa in a 13-year-old child, who had previously undergone surgery because of congenital pes equinovarus.

CONCLUSIONS

In terms of morphometric parameters, the popliteal fossa in the human foetus displays neither male-female nor right-left differences.

In the popliteal fossa, growth patterns of its 4 boundaries, vertical and transverse diameters, and projection surface area all follow natural logarithmic functions.

All the morphometric data considered age-specific reference intervals, which may be conducive in the diagnostics of congenital abnormalities in the human foetus.

ARTICLE INFORMATION AND DECLARATIONS

Ethics statement

The present examinations were ethically approved by the Bioethics Committee of the Ludwik Rydygier Collegium Medicum in Bydgoszcz and the Nicolaus Copernicus University in Bydgoszcz.

Authors' contributions

Mateusz Badura: concept, dissection, collecting data, statistical analysis, literature search, writing the article. **Maria Dąbrowska:** concept, dissection, collecting data, statistical analysis, literature search, writing the article. **Anna Badura:** statistical analysis, literature search. **Monika Paruszevska-Achtel:** dissection, literature search, writing the article. **Magdalena Grzonkowska:** dissection, literature search. **Mariusz Baumgart:** dissection, collecting data, statistical analysis. **Michał Szpinda:** writing the article, final approval of article.

Funding

None.

Conflict of interest

The authors declare that there is no conflict of interest.

REFERENCES

1. Aktan İkiz ZA, Ucerler H, Ozgur Z. Anatomic variations of popliteal artery that may be a reason for entrapment. *Surg Radiol Anat.* 2009; 31(9): 695–700, doi: [10.1007/s00276-009-0508-9](https://doi.org/10.1007/s00276-009-0508-9), indexed in Pubmed: [19418007](https://pubmed.ncbi.nlm.nih.gov/19418007/).
2. Badura M, Wiśniewski M, Szpinda M, et al. Developmental dynamics of the semimembranosus muscle in human foetuses. *Med Biol Sci.* 2011; 25: 13–16.
3. Badura M, Wiśniewski M, Szpinda M, et al. The growth of the semitendinosus muscle in human foetuses. *Med Biol Sci.* 2011; 25: 17–21.
4. Benninger B, Delamarter T. Distal semimembranosus muscle-tendon-unit review: morphology, accurate terminology, and clinical relevance. *Folia Morphol.* 2013; 72(1): 1–9, doi: [10.5603/fm.2013.0001](https://doi.org/10.5603/fm.2013.0001), indexed in Pubmed: [23749704](https://pubmed.ncbi.nlm.nih.gov/23749704/).
5. Bergman RA. Compendium of human anatomic variation: text, atlas and world literature. Urban & Schwarzenberg, Baltimore 1988.
6. Bergman RA, Walker CW, el-Khour GY. The third head of gastrocnemius in CT images. *Ann Anat.* 1995; 177(3): 291–294, doi: [10.1016/s0940-9602\(11\)80205-0](https://doi.org/10.1016/s0940-9602(11)80205-0), indexed in Pubmed: [7598226](https://pubmed.ncbi.nlm.nih.gov/7598226/).
7. Chason DP, Schultz SM, Fleckenstein JL. Tensor fasciae suralis: depiction on MR images. *AJR Am J Roentgenol.* 1995; 165(5): 1220–1221, doi: [10.2214/ajr.165.5.7572507](https://doi.org/10.2214/ajr.165.5.7572507), indexed in Pubmed: [7572507](https://pubmed.ncbi.nlm.nih.gov/7572507/).
8. Chetty D, Pillay P, Lazarus L, et al. The Common Fibular Nerve (and its Branches) in Fetuses. *Int J Morphol.* 2014; 32(2): 455–460, doi: [10.4067/s0717-95022014000200013](https://doi.org/10.4067/s0717-95022014000200013).
9. Covey DC. Injuries of the posterolateral corner of the knee. *J Bone Joint Surg Am.* 2001; 83(1): 106–118, doi: [10.2106/00004623-200101000-00015](https://doi.org/10.2106/00004623-200101000-00015), indexed in Pubmed: [11205847](https://pubmed.ncbi.nlm.nih.gov/11205847/).
10. Dave MR, Yagain V, Anadkat S. Unilateral third/accessory head of the gastrocnemius muscle: a case report. *Int*

- J Morphol. 2012; 30(3): 1061–1064, doi: [10.4067/s0717-95022012000300048](https://doi.org/10.4067/s0717-95022012000300048).
11. Derzsi Z, Gurzu S, Jung I, et al. Arteriovenous synovial hemangioma of the popliteal fossa diagnosed in an adolescent with history of unilateral congenital clubfoot: case report and a single-institution retrospective review. *Rom J Morphol Embryol*. 2015; 56(2): 549–552, indexed in Pubmed: [26193227](https://pubmed.ncbi.nlm.nih.gov/26193227/).
 12. Dudek K, Kędzia W, Kędzia E, et al. Mathematical modeling of the growth of human fetus anatomical structures. *Anat Sci Int*. 2017; 92(4): 521–529, doi: [10.1007/s12565-016-0353-y](https://doi.org/10.1007/s12565-016-0353-y), indexed in Pubmed: [27393150](https://pubmed.ncbi.nlm.nih.gov/27393150/).
 13. Grzonkowska M, Badura M, Lisiecki J, et al. Growth dynamics of the triceps brachii muscle in the human fetus. *Adv Clin Exp Med*. 2014; 23(2): 177–184, doi: [10.17219/acem/37045](https://doi.org/10.17219/acem/37045), indexed in Pubmed: [24913107](https://pubmed.ncbi.nlm.nih.gov/24913107/).
 14. Iwai T, Sato S, Yamada T, et al. Popliteal vein entrapment caused by the third head of the gastrocnemius muscle. *Br J Surg*. 1987; 74(11): 1006–1008, doi: [10.1002/bjs.1800741117](https://doi.org/10.1002/bjs.1800741117), indexed in Pubmed: [3690223](https://pubmed.ncbi.nlm.nih.gov/3690223/).
 15. Kadir D, Ceren U, Busra S, et al. A study on the structure and morphologic development of calcaneal tendon and triceps surae muscle in human fetuses during the fetal period and the evaluation of clinical importance of calcaneal tendon. *Int J Morphol*. 2015; 33(3): 920–929, doi: [10.4067/s0717-95022015000300019](https://doi.org/10.4067/s0717-95022015000300019).
 16. Kim DI, Kim HJ, Shin C, et al. An abnormal muscle in the superficial region of the popliteal fossa. *Anat Sci Int*. 2009; 84(1-2): 61–63, doi: [10.1007/s12565-008-0002-1](https://doi.org/10.1007/s12565-008-0002-1), indexed in Pubmed: [19214656](https://pubmed.ncbi.nlm.nih.gov/19214656/).
 17. Kotian SR, Sachin KS, Bhat KMR. Bifurcated plantaris with rare relations to the neurovascular bundle in the popliteal fossa. *Anat Sci Int*. 2013; 88(4): 239–241, doi: [10.1007/s12565-013-0184-z](https://doi.org/10.1007/s12565-013-0184-z), indexed in Pubmed: [23771697](https://pubmed.ncbi.nlm.nih.gov/23771697/).
 18. Liu H, Fletcher J, Garrison MK, et al. Bilateral absence of quadratus femoris and semimembranosus. *Int J Anat Var*. 2011; 4: 40–42.
 19. Montet X, Sandoz A, Mauget D, et al. Sonographic and MRI appearance of tensor fasciae suralis muscle, an uncommon cause of popliteal swelling. *Skeletal Radiol*. 2002; 31(9): 536–538, doi: [10.1007/s00256-002-0496-x](https://doi.org/10.1007/s00256-002-0496-x), indexed in Pubmed: [12195508](https://pubmed.ncbi.nlm.nih.gov/12195508/).
 20. Okamoto K, Wakebe T, Saiki K, et al. An anomalous muscle in the superficial region of the popliteal fossa, with special reference to its innervation and derivation. *Ann Anat*. 2004; 186(5-6): 555–559, doi: [10.1016/S0940-9602\(04\)80106-7](https://doi.org/10.1016/S0940-9602(04)80106-7), indexed in Pubmed: [15646291](https://pubmed.ncbi.nlm.nih.gov/15646291/).
 21. Olewnik Ł, Podgórski M, Polgaj M, et al. The plantaris muscle — rare relations to the neurovascular bundle in the popliteal fossa. *Folia Morphol*. 2018; 77(4): 785–788, doi: [10.5603/FM.a2018.0039](https://doi.org/10.5603/FM.a2018.0039), indexed in Pubmed: [29651792](https://pubmed.ncbi.nlm.nih.gov/29651792/).
 22. Rowicki K, Płomiński J, Bachta A. Evaluation of the effectiveness of platelet rich plasma in treatment of chronic pes anserinus pain syndrome. *Ortop Traumatol Rehabil*. 2014; 16(3): 307–318, doi: [10.5604/15093492.1112532](https://doi.org/10.5604/15093492.1112532), indexed in Pubmed: [25058106](https://pubmed.ncbi.nlm.nih.gov/25058106/).
 23. Sinav A, Gümüşalan Y, Arifoğlu Y, et al. Accessory muscular bundles arising from biceps femoris muscle. *Kaibogaku Zasshi*. 1995; 70(3): 245–247, indexed in Pubmed: [7645372](https://pubmed.ncbi.nlm.nih.gov/7645372/).
 24. Spina AA. The plantaris muscle: anatomy, injury, imaging, and treatment. *J Can Chiropr Assoc*. 2007; 51(3): 158–165, indexed in Pubmed: [17885678](https://pubmed.ncbi.nlm.nih.gov/17885678/).
 25. Standring S. *Gray's Anatomy: the anatomical basis of clinical practice*. 44th ed. Elsevier, London 2021.
 26. Sussmann AR. Congenital bilateral absence of the semimembranosus muscles. *Skeletal Radiol*. 2019; 48(10): 1651–1655, doi: [10.1007/s00256-019-03210-3](https://doi.org/10.1007/s00256-019-03210-3), indexed in Pubmed: [30982941](https://pubmed.ncbi.nlm.nih.gov/30982941/).
 27. Szpinda M. *Anatomia prawidłowa człowieka*. vol. 1. Edra Urban & Partner, Wrocław 2022.
 28. Szpinda M, Paruszevska-Achtel M, Dąbrowska M, et al. The normal growth of the biceps brachii muscle in human fetuses. *Adv Clin Exp Med*. 2013; 22(1): 17–26, indexed in Pubmed: [23468258](https://pubmed.ncbi.nlm.nih.gov/23468258/).
 29. Szpinda M, Wiśniewski M, Rolka Ł. The biceps femoris muscle in human fetuses — a morphometric, digital and statistical study. *Adv Clin Exp Med*. 2011; 20(5): 575–582.
 30. Tubbs RS, Caycedo FJ, Oakes WJ, et al. Descriptive anatomy of the insertion of the biceps femoris muscle. *Clin Anat*. 2006; 19(6): 517–521, doi: [10.1002/ca.20168](https://doi.org/10.1002/ca.20168), indexed in Pubmed: [16283645](https://pubmed.ncbi.nlm.nih.gov/16283645/).
 31. Weschenfelder W, Lindner R, Spiegel C, et al. Desmoid tumor of the popliteal fossa during pregnancy. *Case Rep Surg*. 2015; 2015: 262654, doi: [10.1155/2015/262654](https://doi.org/10.1155/2015/262654), indexed in Pubmed: [25734019](https://pubmed.ncbi.nlm.nih.gov/25734019/).
 32. Yıldız S, Kocabıyık N, Çilingiroğlu S, et al. Morphometry of plantaris muscle in human fetuses. *Gülhane Tıp Dergisi*. 2011; 53(3): 149–153.